

## Supporting Information

### **Title : Dually Prewetted Membrane for Continuous Filtrate of Water-in-Light Oil, Oil-in-Water and Water-in-Heavy Oil Multiphase Emulsion Mixtures**

*Guoliang Cao, Yonggui Wang,<sup>†</sup> Chengyu Wang<sup>\*†</sup> and Shih-Hsin Ho<sup>\*‡</sup>*

<sup>†</sup>Key Laboratory of Bio-Based Material Science and Technology of Ministry of Education, Northeast Forestry University, Harbin, 150040, P. R. China

<sup>‡</sup>State Key Laboratory of Urban Water Resource and Environment, Harbin Institute of Technology, Harbin, 150040, P. R. China

Email: wangcy@nefu.edu.cn; stephen6949@hit.edu.cn

Keywords: underwater superoleophobicity, underoil superhydrophobicity, dually prewetted, continuous separation, multiphase emulsion.

#### **This file includes:**

Materials

Experimental Procedures

Figures S1 to S7

\*To whom all correspondence should be addressed Electronic mail:

Chengyu Wang: wangcy@nefu.edu.cn

Shih-Hsin Ho: stephen6949@hit.edu.cn

**Materials.** Synthetic CB Degussa (Evonik) FW200 (surface area 460 m<sup>2</sup>/g, average diameter 13 nm) was purchased. Methylbenzene, dimethylbenzene, hexane, chloroform, tetrachloromethane, dichloroethane and absolute ethanol were purchased from Guangdong Guanghua Sci-Tech Co., Ltd. (Guangdong, China). Span 80 and Tween 80 were purchased from Shanghai Aladdin Bio-Chem Technology Co., Ltd. (Shanghai, China). An Ultrapure Water System was provided by Beijing Zhongyang Yongkang Environmental Protection Technology Co., Ltd. (Beijing, China). All reagents were used as-received without further purification. LIVE/DEAD<sup>®</sup> BacLight<sup>™</sup> bacterial viability kit (Molecular Probes, L-7012). calcofluor-white stain (fluorescent brightener 28; Sigma-Aldrich, St Louis, MO, USA). A Millipore PVDF microfiltration membrane with an average pore size of 0.45 μm was used.

The chemical composition of the DCBM was assessed by Fourier transform infrared spectroscopy (FT-IR).<sup>[1]</sup> As shown in figure S1, line Black is the PVDF membrane, peak at 1173 cm<sup>-1</sup>, which stem from C-F<sub>2</sub> stretching vibrations. Peaks centered around 3023, 2980 and 1734 cm<sup>-1</sup> represented obvious C-H and C=O stretching vibration. The peaks at 1403 and 876 cm<sup>-1</sup> were designated as a C-C skeleton vibration. Line Red in figure S1 were the FT-IR spectroscopy of the DCBM, the peak at 1706 cm<sup>-1</sup> is due to hydrogen-bonded C=O stretching indicating that the CB disturbed the C=O due to the strong interaction between CB and PU.<sup>[2]</sup> Peaks around 1210 cm<sup>-1</sup> is C-N stretching vibration and N-H bending. Peaks around 1514-1561 cm<sup>-1</sup> are N-H formation vibration C-N and C-C stretching vibration, sensitive to chain conformation and intermolecular hydrogen bonding. Weak peaks at 2780-2887 cm<sup>-1</sup> represented an obvious C-H stretching vibration on account of PU and CB. Double peaks at 2118 and 2085 cm<sup>-1</sup> represented an obvious C≡C stretching vibration on account of CB.

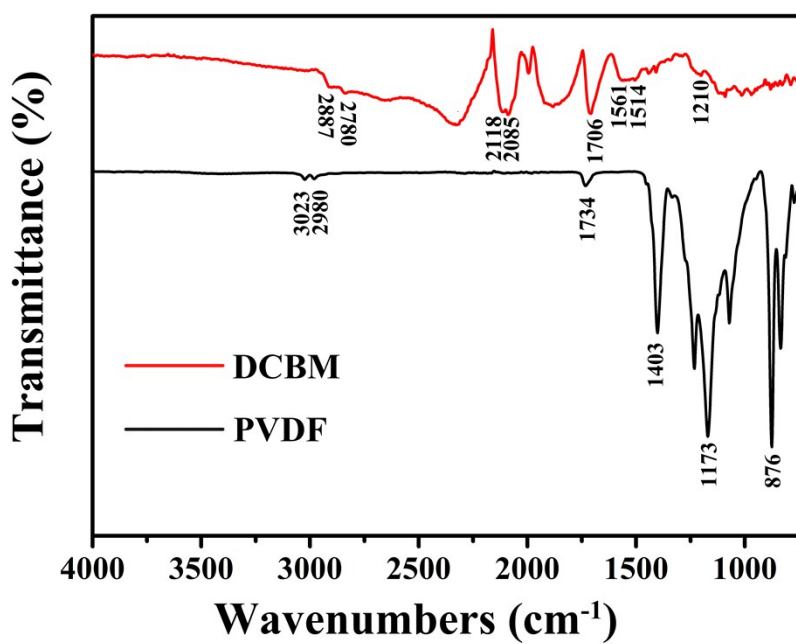


Figure S1. FT-IR spectroscopy of DCBM and PVDF

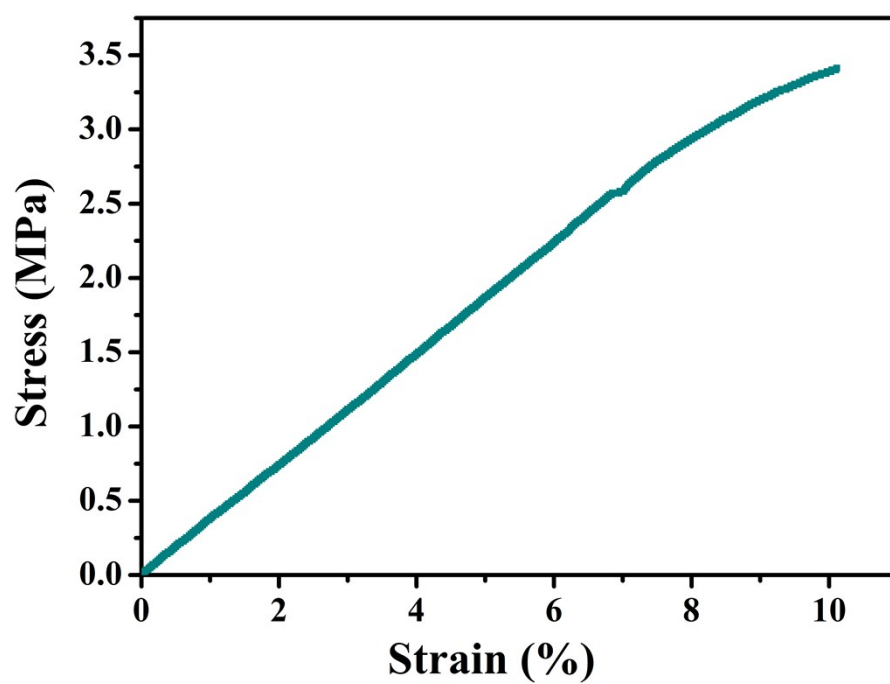
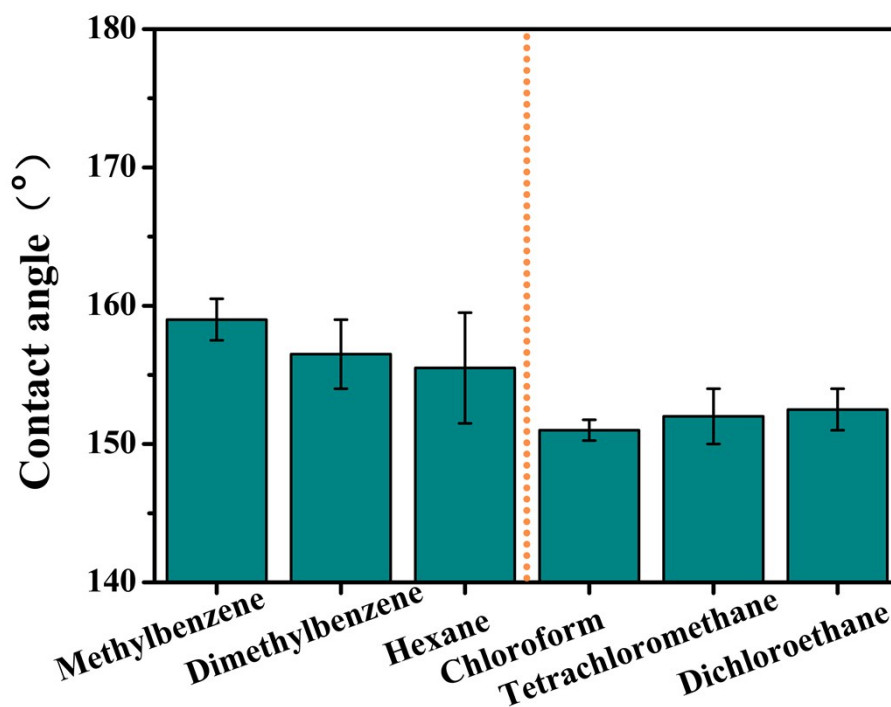


Figure S2. Stress-strain curves of the DCBM.



**Figure S3.** The contact angles of water droplets under several types of oils (left) and oil droplets underwater (right) on the DCBM.

**Separation of water-in-light oil, oil-in-water and water-in-heavy oil three-phase emulsion mixtures.**

The half of DCBM first prewetted with water by dropper to comprise a water-containing region (WCR) and successively the other half of DCBM prewetted with corresponding heavy oil by the other dropper to comprise an oil-containing region (OCR).

Then, the DCMB was fixed between two frosted glass fixtures: the upper frosted glass fixture was connected to a glass container, and the lower frosted glass fixture had two outlets, each attached to a glass tube. The two glass guide tubes were placed beneath the WCR and the

OCR. Six types of water-in-light oil, oil-in-water and water-in-heavy oil three-phase emulsion mixtures were investigated in this study, including: water-in-methylbenzene/methylbenzene-

in-water/water-in-chloroform (E1), water-in-dimethylbenzene/dimethylbenzene-in-water/water-in-tetrachloromethane (E2), water-in-hexane/hexane-in-water/water-in-

dichloroethane (E3), water-in-methylbenzene/chloroform-in-water/water-in-chloroform (E4),

water-in-methylbenzene/tetrachloromethane-in-water/water-in-chloroform (E5) and water-in-

methylbenzene/dichloroethane-in-water/water-in-chloroform (E6). The oils and water were

spiked with Sudan III and methylene blue, respectively. First, the water-in-light oil, oil-in-water and water-in-heavy oil three-phase emulsion mixtures (30 mL, volume ratio = 1:1:1) were added to the upper glass container prior to beginning the separation process with the prewetted DCMB. The DCBM separation efficiency toward the emulsion mixtures were measured according to:  $\eta (\%) = (C1-C2)/C1 \times 100$ , where  $C1$  and  $C2$  are the dispersed phase concentrations of the emulsion (oil concentration for oil-in-water emulsions or water concentration for water-in-oil emulsions) before the separation process and the collected permeate solutions after the separation process. The DCBM emulsion mixture flux was also measured according to  $F = V/S_t$ , where  $V$  is the volume of water or oils that permeate the DCMB, and was set at 10 mL;  $S$  is the effective area of the DCMB and  $t$  is the requisite time for infiltration of 10 mL liquid. The emulsion mixture separation process was vacuum driven by only a pressure of  $-0.01$  MPa (vacuum degree  $-0.01$  MPa).

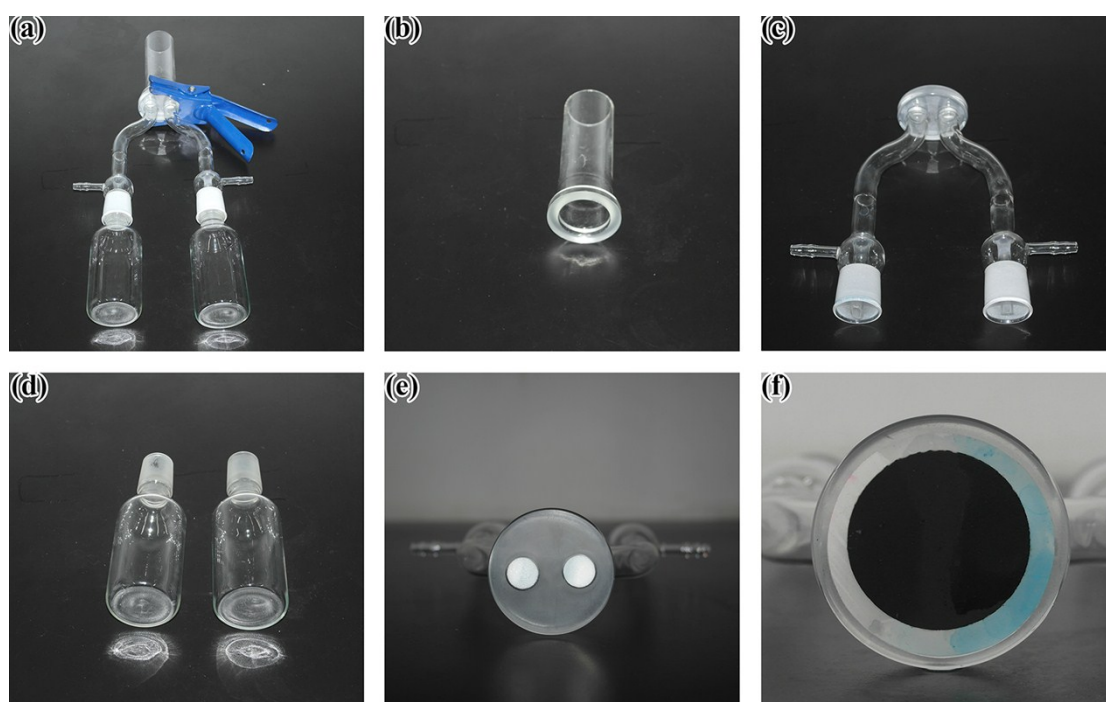


**Figure S4.** (a) DCBM was fixed between two frosted glass fixtures. (b) The upper frosted glass fixture was connected to a glass container. (c) The lower frosted glass fixture had two outlets, each attached to a glass tube. (d) The collected permeate solutions container. (e) The position of two outlets were placed in lower frosted glass fixture. (f) DCBM was placed on

lower frosted glass fixture. DCBM were prewetted by both water and oil, the left of DCBM is oil-containing region (OCR), and the right of DCBM is water-containing region (WCR).

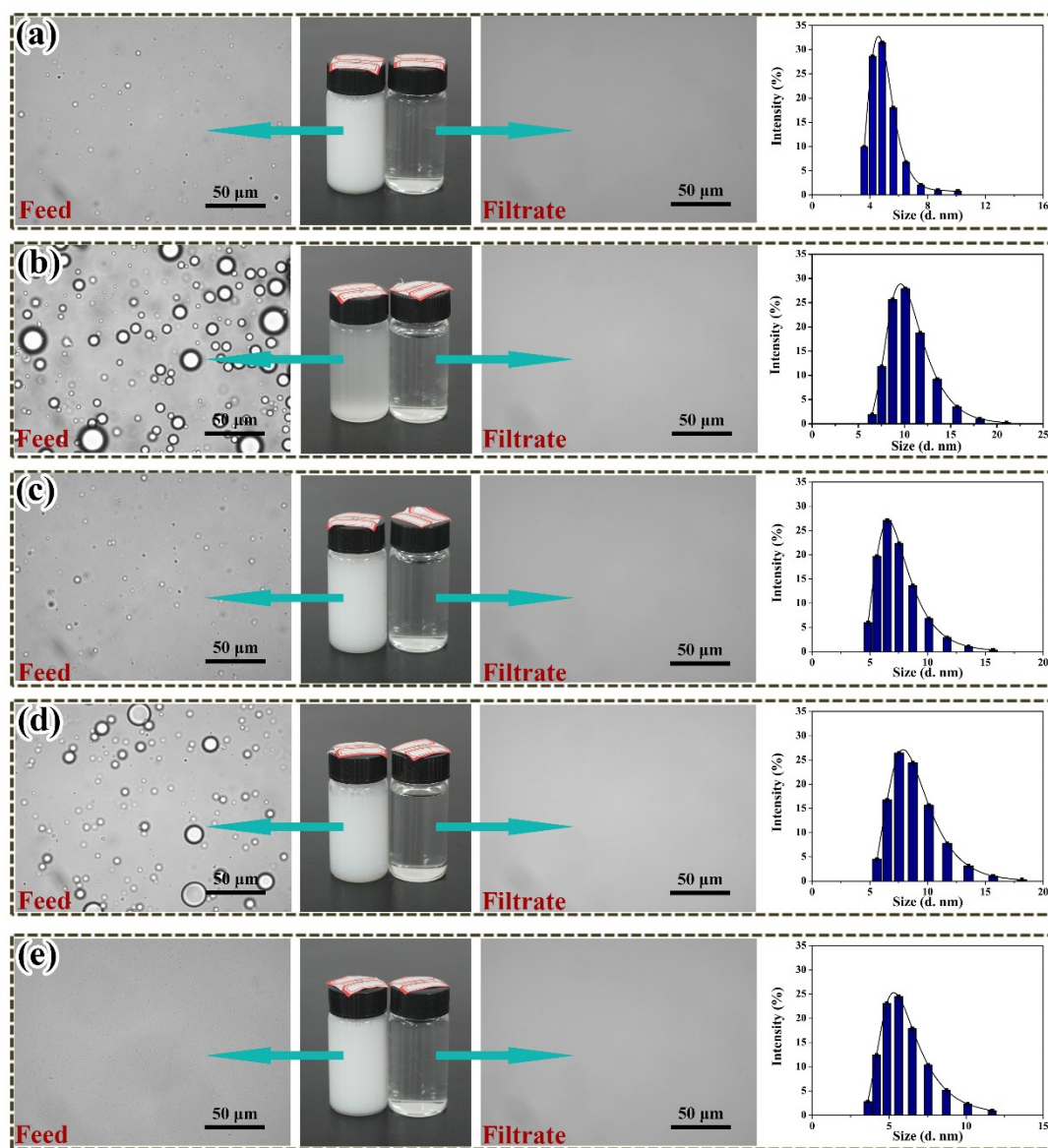


**Figure S5.** (a-e) Left five pictures are the optical microscope images and the digital images of the dimethylbenzene-in-water, hexane-in-water, chloroform-in-water, tetrachloromethane-in-water, dichloroethane-in-water emulsions before and after separation; right is droplet size distribution by DLS.

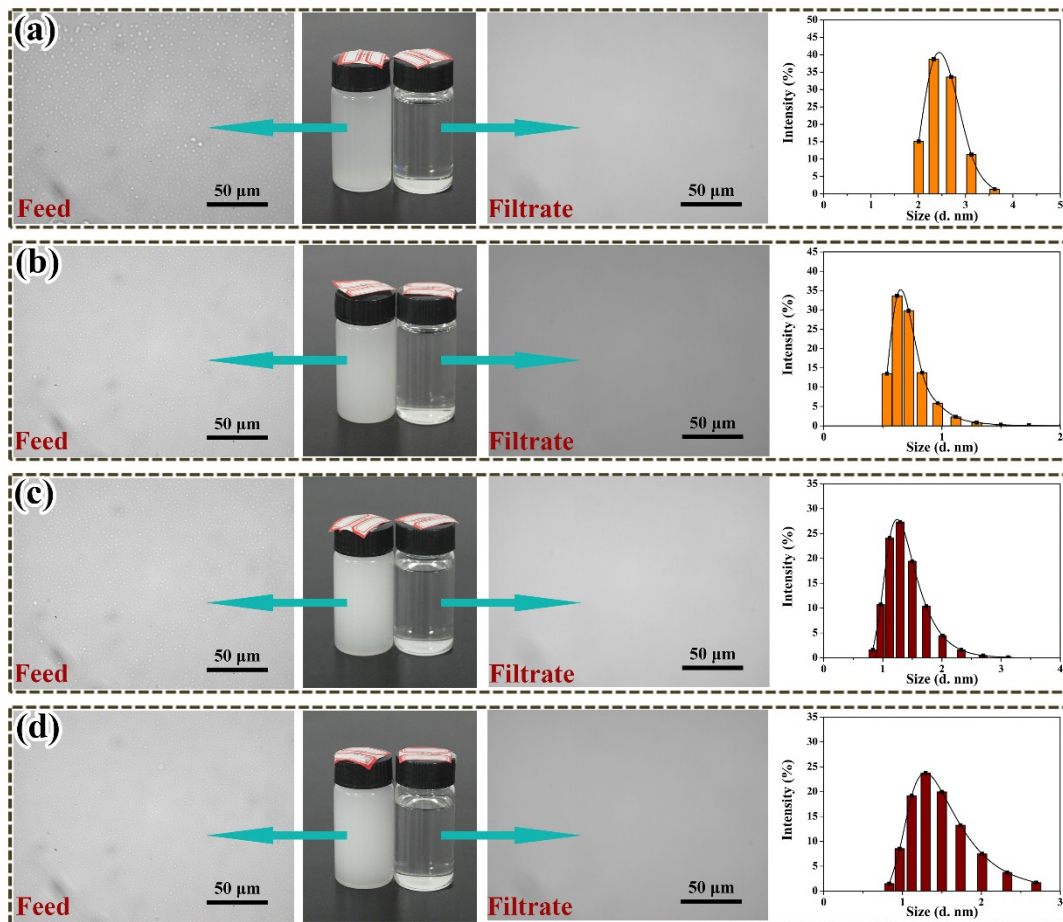


**Figure S6.** (a-c) Left four pictures are the optical microscope images and the digital images of the water-in-dimethylbenzene, water-in-hexane, water-in-tetrachloromethane, water-in-dichloroethane emulsions before and after separation; right is droplet size distribution by DLS.

The DCBM also showed stable underwater superoleophobicity and underoil superhydrophobicity towards many corrosive water solutions (1 M HCl, 1 M NaOH and 1M NaCl), As shown in Fig. S7, contact angles were all larger than  $150^\circ$ . The flux and separation efficiency for corrosive water solutions of the D/W, W/D and W/T emulsions also exhibited extremely stable high fluxes and more than 99% separation efficiency. The results show that DCBM was chemically resistant to the extreme environment conditions.

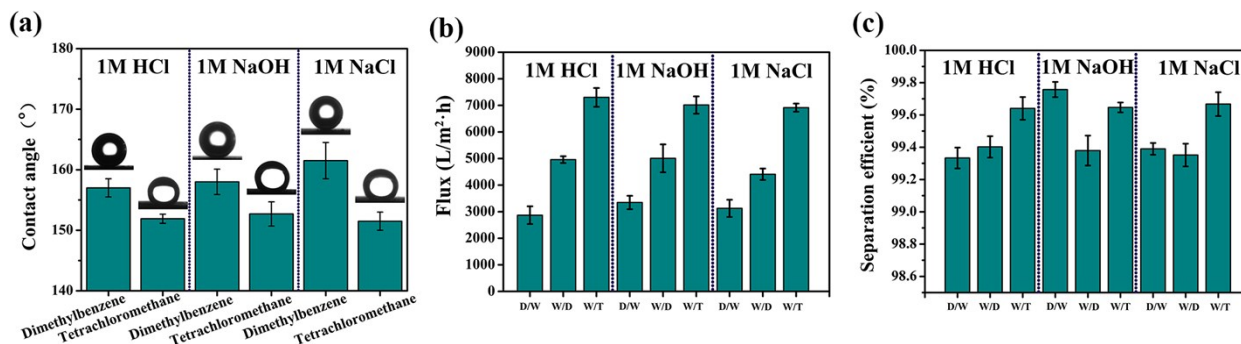


**Figure S7.** (a) The contact angles of corrosive water droplets (HCl NaOH and NaCl) under dimethylbenzene and tetrachloromethane underwater on the DCBM. (b) The flux for corrosive water of the D/W, W/D and W/T emulsions. (c) The separation efficiency for corrosive water of the D/W, W/D and W/T emulsions.

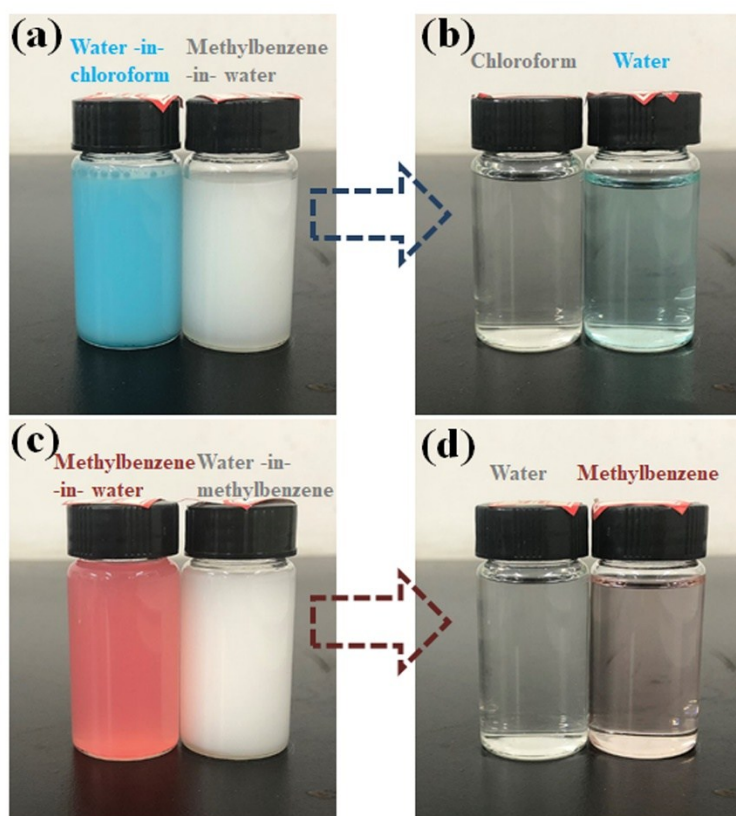


**Figure S8.** (a-b) Physical picture of separation of the methylbenzene-in-water and blue water-in-chloroform two-phase emulsions mixtures. (f-g) Physical picture of separation of the water-in- methylbenzene and methylbenzene-in-water two-phase emulsions mixtures.



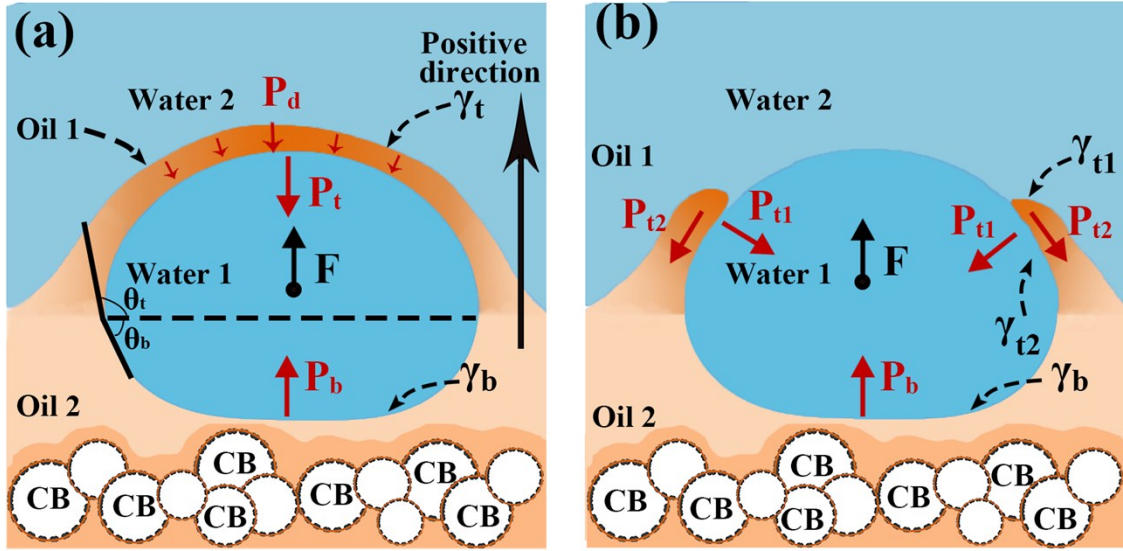


**Figure S9.** Schematic of fouling mechanism for DCBM.

The stabilization of water droplets at the water/heavy oil interface could be attributed to the existence of an ultrathin heavy oil film (oil phase 1) between the water phases 1 and 2. Here, the oil phase 1 is also referred to as the disjoining layer, described by the augmented Young-Laplace equation<sup>[3]</sup> as:

$$P_t = \frac{2\gamma^{w1/o1}\cos\theta_t}{r_t} + P_d$$

Where  $P_t$  is the capillary pressure (difference in pressure between water phase 1 and oil phase 2), which is negative for convex surface.  $\gamma^{w1/o1}$  is the interfacial tension between water phase 1 and oil phase 1,  $\theta_t$  is the contact angle between water phase 1 and oil phase 1,  $r_t$  is the water droplet radius of curvature associated with oil phase 1, and  $P_d$  is the disjoining pressure

in oil phase 1.  $\frac{2\gamma^{w1/o1}\cos\theta_t}{r_t}$  is the pressure caused by the surface curvature between water phase 1 and oil phase 1. Disjoining pressure results from the interaction between van der Waals forces and the electrostatic double-layer when the oil film thickness is  $<100$  nm. At a

given fluid temperature and chemical composition, the disjoining pressure depends on the thickness and the geometry of the film,<sup>[4]</sup> and is described as:

$$P_d = \frac{A(4 - 3h_x^2 + 3hh_{xx})}{24\pi h^3}$$

where  $A$  is the Hamaker constant for water phases 1 and 2 interacting through oil phase 1,  $h$ ,  $h_x$  and  $h_{xx}$  are the oil film thickness, slope and second order derivative of the films, respectively. The two interfaces, that is water phase 1/oil phase 1 and oil phase 1/water phase 2, are approximately parallel, therefore,  $h_x = h_{xx} = 0$  and the disjoining pressure is reduced to:

$$P_d = \frac{A}{6\pi h^3}$$

The difference in pressure at the bottom of the water droplet curvature is given by:

$$P_b = -\frac{2\gamma^{w1/o2}\cos\theta_b}{r_b}$$

where  $\gamma^{w1/o2}$  is the interfacial tension between water phase 1 and oil phase 2,  $\theta_b$  is the contact angle between water phase 1 and oil phase 2,  $r_b$  is the radius of curvature of the water droplet at oil phase 2. The force ( $F$ ), caused by gravity ( $G$ ) and buoyancy ( $F_{buoy}$ ), is given by:  $F = F_{buoy} - G$ . The water droplet (water phase 1) on the thin oil film (oil phase 1) is stable as a result of balancing various forces:

$$F + P_t S_t + P_b S_b = 0$$

where  $S_t$  and  $S_b$  are the interfacial areas of the water droplet at two oil interfaces. When  $h$  is large, the disjoining pressure is small, thus  $P_b + P_t < 0$ , and  $P_b + P_t$  is not able to balance the upward force  $F$ , leading to the rupture of the oil film. When the oil film (oil phase 1) is thinner than the critical thickness  $h_c$ , the disjoining pressure is large, leading to an increase of

$P_b$  and a stable water droplet at the water/oil interface. Finally, large water droplets accumulate and can easily detach from the low-adhesion DCBM surface in the presence of flowing water.

#### References:

- [1] F. Z. Chen, Y. Lu, X. Liu, J. L. Song, G. J. He, M. K. Tiwari, C. J. Carmalt, I. P. Parkin, *Adv. Funct. Mater.* **2017**, 27.
- [2] D. K. Chattopadhyay, A. K. Mishra, B. Sreedhar, K. V. S. N. Raju, *Polym. Degrad. Stabil.* **2006**, 91, 1837.
- [3] S. Dasgupta, J. A. Schonberg, I. Y. Kim, P. C. Wayner, *J. Colloid Interf. Sci.* **1993**, 157, 332.
- [4] a) J. K. Ferri, P. A. L. Fernandes, J. T. McRuiz, F. Gambinossi, *Soft Matter*. **2012**, 8, 10352;  
b) G. Soligno, M. Dijkstra, R. van Roij, *J. Chem. Phys.* **2014**, 141.